Theory and Experiment of Dual-Mode Microstrip Triangular Patch Resonators and Filters

Jia-Sheng Hong, *Member, IEEE,* and Shuzhou Li

***Abstract*—In this paper, we report on the results of an investigation into dual-mode operation of microstrip triangular patch resonators and their applications for designing dual-mode bandpass filters. It has been found theoretically that the dual modes can result from the rotation and superposition of a fundamental mode. The characteristics of the dual modes and their mode splitting are described. The applications of this new type of dual-mode microstrip patch resonator in the design of microwave planar filter are presented. A circuit model for operation of this type of filter is proposed. Two- and four-pole filters of this type are demonstrated for the first time. Both theoretical and experimental results are presented.**

***Index Terms*—Dual-mode filters, dual-mode resonators, microstrip filters, microstrip resonators.**

I. Introduction

MICROSTRIP filters have found wide applications in many RF/microwave circuits and systems. This is particularly driven by rapidly growing wireless communications, emerging high-temperature superconducting (HTS), and micromachining technologies [1]–[7]. In general, microstrip bandpass filters may be designed using single- or dual-mode resonators. Dual-mode microstrip resonators are attractive because each of the dual-mode resonators can be used as a doubly tuned resonant circuit and, therefore, the number of resonators required for a given degree filter is reduced by half, resulting in a compact filter configuration [7]–[11].

Several types of dual-mode microstrip resonators have been used, including the circular ring [8], meander loop [9], circular disk, and square patch [10], [11]. The one-dimensional (1-D) transmission-line dual-mode resonators such as rings and loops are smaller in size than the two-dimensional (2–D) patch dual-mode resonators such as circular disks and square patches. However, the line-based resonators generally suffer from higher conductor loss and lower power-handling capability. Therefore, the patch resonators appear more attractive for bandpass filter applications where low insertion loss and high power handling are of primary concern [12]–[15]. In addition, at millimeter waves, the size may not be the issue and the use of patch resonators can also ease the fabrication.

Manuscript received September 10, 2003; revised November 11, 2003.

J.-S. Hong is with the Department of Electrical, Electronic, and Computer Engineering, School of Engineering and Physical Sciences, Heriot-Watt University, Edinburgh EH14 4AS, U.K. (e-mail: J.Hong@hw.ac.uk).

S. Li was with the Department of Electrical, Electronic, and Computer Engineering, School of Engineering and Physical Sciences, Heriot-Watt University, Edinburgh EH14 4AS, U.K., on leave from the Institute of Acoustics, Chinese Academy of Sciences, Beijing 100080, China.

Digital Object Identifier 10.1109/TMTT.2004.825653

However, thus far, only a few dual-mode microstrip patch resonators, i.e., square and circular patches, have been available for the filter design. Although microstrip filters using triangular patch resonators have been reported recently [15], each of the triangular patches operates merely with a single mode at a certain frequency band. The triangular patch is an interesting element. However, up to date, only single-mode operations have been reported [15]–[17], [19].

In this paper, we report on the latest research results into the dual-mode operation of triangular patch resonators and their applications for designing dual-mode filters [18]. In Section II, the theoretical solutions have been derived for the first time to show the dual-mode operation of an equilateral triangular microstrip patch resonator. For the applications of this new dual-mode patch resonator, it is desirable to visualize the field patterns of the operated modes, which is presented in Section III. Section IV deals with the applications for designing dual-mode microstrip triangular patch resonator filters. The mode-splitting characteristics of two fundamental degenerate modes are described. A circuit model is proposed for the operation of this type of dual-mode filter. Dual-mode microstrip bandpass filters, two two-pole and one four-pole filters of this type, are demonstrated theoretically and experimentally for the first time. Finally, conclusions are given in Section V.

II. Theoretical Formulation

Fig. 1 shows the geometry of an equilateral triangular microstrip patch resonator on a dielectric substrate with a ground plane. Similar to dealing with a square patch microstrip resonator [1], a Wheeler's cavity mode can be used, where the top and bottom of the cavity are the perfect electric walls and the remaining sides are the perfect magnetic walls. One can then expand the electromagnetic (EM) fields inside the triangular cavity in terms of $\mathrm{TM}^z_{m,n,l}$ modes [16]

$$\begin{aligned} E_z(x,y) &= A_{m,n,l}\left\{\cos\left[\left(\frac{2\pi x}{\sqrt{3}a}+\frac{2\pi}{3}\right)l\right]\cos\left[\frac{2\pi(m-n)y}{3a}\right]\right. \\ &\quad +\cos\left[\left(\frac{2\pi x}{\sqrt{3}a}+\frac{2\pi}{3}\right)m\right]\cos\left[\frac{2\pi(n-l)y}{3a}\right] \\ &\quad \left.+\cos\left[\left(\frac{2\pi x}{\sqrt{3}a}+\frac{2\pi}{3}\right)n\right]\cos\left[\frac{2\pi(l-m)y}{3a}\right]\right\} \\ H_x &= \frac{j}{\omega\mu_0}\frac{\partial E_z}{\partial y} \\ H_y &= \frac{-j}{\omega\mu_0}\frac{\partial E_z}{\partial x} \end{aligned} \tag{1}$$

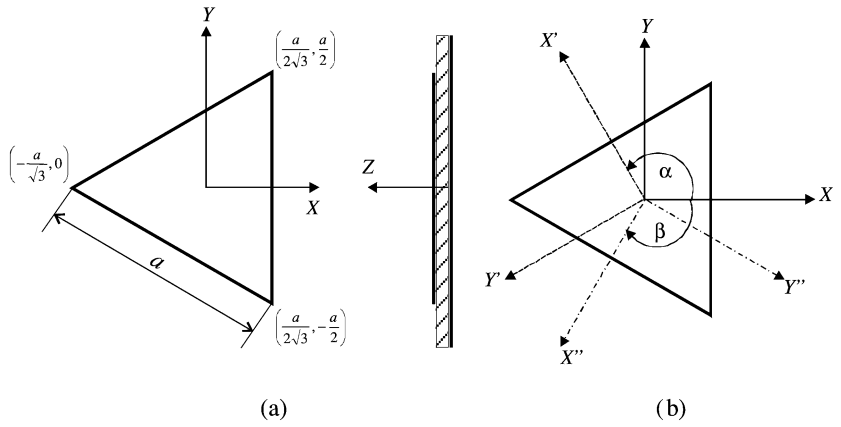

Fig. 1. (a) Equilateral triangular microstrip patch geometry. (b) Rotated coordinate systems.

where $A_{m,n,l}$ is a constant and a is the length of the triangle side. Note that for the $\mathrm{TM}^z_{m,n,l}$ modes $H_z = E_x = E_y = 0$. Unlike the square patch resonator, the indexes $m, n,$ and l in (1) do not represent the number of standing waves along the $x, y,$ and z axes of the coordinate system, and the condition of $m + n + l = 0$ must also be imposed to satisfy the wave equation. A fundamental mode, which can be found from (1), is the $\mathrm{TM}^z_{1,0,-1}$ mode and its electric field is given by

$$E_z(x,y) = A_{1,0,-1}\left\{2\cos\left(\frac{2\pi x}{\sqrt{3}a} + \frac{2\pi}{3}\right)\cos\left(\frac{2\pi y}{3a}\right) + \cos\left(\frac{4\pi y}{3a}\right)\right\}. \quad (2)$$

However, our intention is to find out another degenerate mode to pair with (2). It is well known that $\mathrm{TM}^z_{1,0,0}$ and $\mathrm{TM}^z_{0,1,0}$ are a pair of degenerate modes of a square patch resonator [1]. A question then arises is as follows: by similarity, would the $\mathrm{TM}^z_{0,1,-1}$ mode be another degenerate mode of an equilateral triangular patch resonator? Unfortunately, the problem we are facing is not as simple as that, and the answer to the question also is not. The reason is as follows: by inspection of (1), we notice that the interchange of the three indexes $m, n,$ and l in (1) leaves the field patterns are unchanged. Hence, the EM fields for $\mathrm{TM}^z_{0,1,-1}$, as well as $\mathrm{TM}^z_{-1,0,1}$ and $\mathrm{TM}^z_{0,-1,1}$ modes, which all have the same resonant frequency as that of the $\mathrm{TM}^z_{1,0,-1}$ mode, are exactly identical to that given in (2). It is envisaged that (1) alone cannot predict any degenerate modes, which have the same resonant frequency, but different field patterns to that given by (2). This is because the EM field solutions of (1) are, as a matter of fact, not a complete set. To investigate degenerate modes theoretically, we have used the following formulation.

For our purpose, let us consider the dominant mode only, and express the vector fields in the (x, y, z) coordinate system

$$\begin{aligned}\underline{E} &= E_z(x,y)\hat{z}\\ \underline{H} &= H_x(x,y)\hat{x} + H_y(x,y)\hat{y}\end{aligned} \quad (3)$$

where $E_z(x, y)$ is given by (2), and all the magnetic-field components can be derived from the electric field, as indicated in (1). Noticing a rotation symmetry of the equilateral triangular patch resonator, the vector fields can also be expressed in the two rotated coordinate systems, i.e., the (x', y', z) and (x'', y'', z) coordinate systems, as shown in Fig. 1(b), respectively,

$$\begin{aligned}\underline{E'} &= E'_z(x',y')\hat{z}\\ \underline{H'} &= H'_x(x',y')\hat{x}' + H'_y(x',y')\hat{y}'\end{aligned} \quad (4)$$

$$\begin{aligned}\underline{E''} &= E''_z(x'',y'')\hat{z}\\ \underline{H''} &= H''_x(x'',y'')\hat{x}'' + H''_y(x'',y'')\hat{y}''\end{aligned} \quad (5)$$

where $E'_z(x', y')$ and $E''_z(x'', y'')$ take the same form as (2) in the associated coordinate systems. By far, neither set of the field solutions of (3)–(5) alone can predict any degenerate-mode operation. However, if there is another degenerate mode other than (2) existing in the (x, y, z) coordinate system, it must result from, according to the principle of superposition, a superposition of these fields. In this way, we have found that

$$\begin{aligned}&\underline{E'} - \underline{E''}\\ &\underline{H'} - \underline{H''}\end{aligned} \quad (6)$$

is indeed a field solution for the other fundamental degenerate mode.

In order to present this newly found degenerate mode in the (x, y, z) coordinate system, we need to first project the vector fields of (6) onto the (x, y, z) coordinate systems with the following transformations:

$$\begin{aligned}\hat{x}' &= \hat{x}\cos(\alpha) + \hat{y}\sin(\alpha)\\ \hat{y}' &= -\hat{x}\sin(\alpha) + \hat{y}\cos(\alpha)\\ \hat{x}'' &= \hat{x}\cos(\beta) + \hat{y}\sin(\beta)\\ \hat{y}'' &= -\hat{x}\sin(\beta) + \hat{y}\cos(\beta)\end{aligned} \quad (7)$$

where $\alpha = 2\pi/3$ and $\beta = -2\pi/3$ are the coordinate rotating angles, which are indicated in Fig. 1(b). Similarly, we also need to express x', y', x'', and y'' in terms of x, y using the same coordinate transformations. The resultant electric field of the

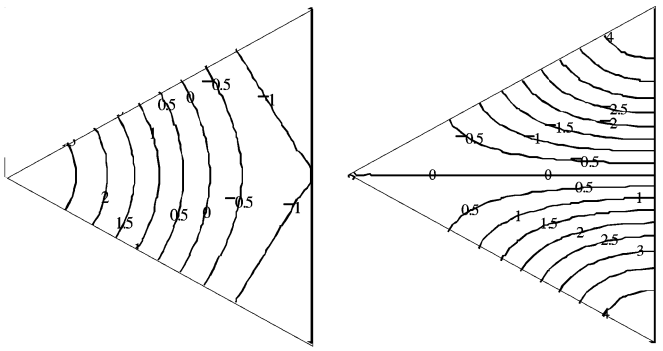

(a) (b)

Fig. 2. Electric-field patterns of the degenerate modes. (a) Mode 1. (b) Mode 2.

newly found degenerate mode, as a counterpart of (2), is given by

$$E'_z(x,y) - E''_z(x,y) = A_{1,0,-1} \begin{cases} 2\cos\left(\dfrac{2\pi(x\cos(\alpha)+y\sin(\alpha))}{\sqrt{3}a}+\dfrac{2\pi}{3}\right) \\ \quad \times \cos\left(\dfrac{2\pi(-x\sin(\alpha)+y\cos(\alpha))}{3a}\right) \\ \quad + \cos\left(\dfrac{4\pi(-x\sin(\alpha)+y\cos(\alpha))}{3a}\right) \\ -2\cos\left(\dfrac{2\pi(x\cos(\beta)+y\sin(\beta))}{\sqrt{3}a}+\dfrac{2\pi}{3}\right) \\ \quad \times \cos\left(\dfrac{2\pi(-x\sin(\beta)+y\cos(\beta))}{3a}\right) \\ \quad - \cos\left(\dfrac{4\pi(-x\sin(\beta)+y\cos(\beta))}{3a}\right). \end{cases} \tag{8}$$

The resultant magnetic fields can be found accordingly. Thus, (2) and (8) give the basic field solutions of a pair of fundamental degenerate modes in an equilateral triangular microstrip patch resonator. We should refer to them as mode 1, which is based on (2), and mode 2, which is based on (8) in the following discussions.

III. Field Patterns of Degenerate Modes

For applications of a microwave resonator, it is always desirable to know the field pattern of a relevant resonant mode. Using the formulation described in Section II, a computer program was written and used to compute the field patterns of the two degenerate modes of a triangular patch resonator. Fig. 2 illustrates the computed electric fields of modes 1 and 2, directly resulting from (2) and (8), respectively. It is interesting to see that mode 1 has a symmetric field with respect to the horizontal axis, whereas mode 2 exhibits an antisymmetric field pattern. One can also observe that the field pattern of either mode cannot be obtained by simply rotating its counterpart's field. This situation is totally different from that of the dual modes of a square or circular patch resonator, where the one mode can be obtained by rotating the other mode by 90° in the coordinate system.

Since the magnetic field $\underline{H}$ can be derived from the electric field, we can find the current distribution or density $\underline{J} = \hat{z} \times \underline{H}$ accordingly. The computed current distributions of the two degenerate modes of an equilateral triangular patch resonator are shown in Fig. 3. Again, we can see that, with respect to the horizontal symmetric plane, modes 1 and 2 behave as an even and odd mode, respectively.

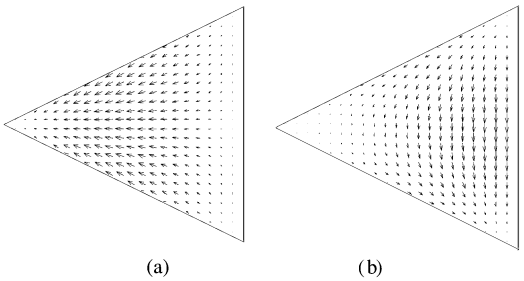

(a) (b)

Fig. 3. Current distributions of the degenerate modes. (a) Mode 1. (b) Mode 2.

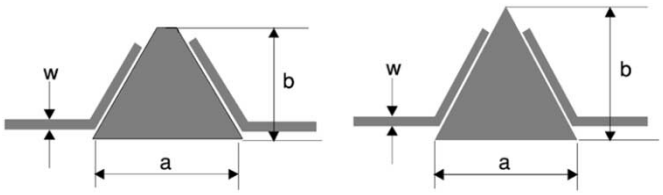

(a) (b)

Fig. 4. Two-pole dual-mode microstrip triangular patch resonator filters. (a) Structure 1. (b) Structure 2.

IV. Dual-Mode Bandpass Filters

To demonstrate the application of the proposed dual-mode microstrip triangular patch resonator, two-pole bandpass filters with a single microstrip triangular patch resonator were investigated first. Two filter structures have been developed, which are depicted in Fig. 4. Note that, for an equilateral triangle, $b = \sqrt{3}a/2$. Since we need to split the two degenerate modes of an equilateral triangular patch resonator for designing a bandpass filter, the mode splitting is achieved by introducing a small cut, as shown in Fig. 4(a), where $b < \sqrt{3}a/2$, or by deforming the equilateral triangle into an isosceles triangle, as shown in the case of Fig. 4(b), where $b \neq \sqrt{3}a/2$. In either case, we found that the resonant frequency of mode 1 was effectively shifted, whereas the resonant frequency of mode 2 was almost unchanged [18]. At first, it was thought that once the modes were split, as is the case for a perturbed square dual-mode patch resonator, there would be some coupling between the two modes [18]. However, after a careful examination of this type of mode splitting, according to the theory of asynchronously tuned coupled resonators (i.e., if the two split-mode frequencies are equal to the two self-resonant frequencies, respectively, there is no coupling between the two resonators [1]), it was then believed that the two modes were actually hardly coupled to each other for the mode perturbations introduced. This discovery is very important for developing a dual-mode filter of this type and understanding its operation.

The equality between the self-resonant frequencies and split-mode frequencies for the geometrical perturbations used has been investigated using full-wave EM simulations, and is demonstrated as follows. By inspecting the field patterns of Figs. 2 and 3, we can see that mode 1 is actually an even mode, while mode 2 is an odd mode. This allows us to simulate the self-resonant frequencies of the two modes

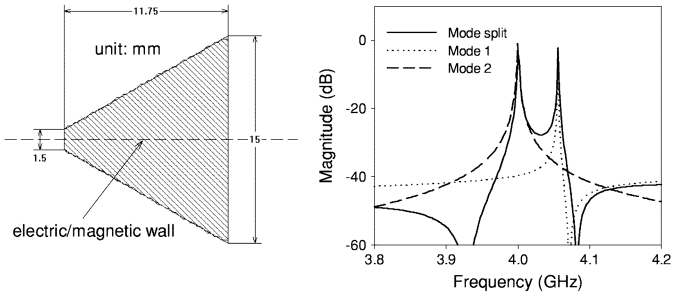

Fig. 5. Simulated split-mode frequencies (full-line) and self-resonant frequencies (dotted line for mode 1 and dashed line for mode 2) for a perturbed (small cut) dual-mode triangular microstrip resonator on a 1.27-mm-thick dielectric substrate with a relative dielectric constant of 10.8.

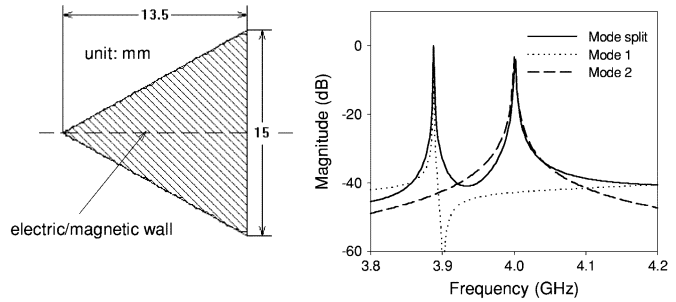

Fig. 6. Simulated split-mode frequencies (full-line) and self-resonant frequencies (dotted line for mode 1 and dashed line for mode 2) for a perturbed (isosceles) dual-mode triangular microstrip resonator on a 1.27-mm-thick dielectric substrate with a relative dielectric constant of 10.8.

by placing a magnetic or electric wall along the symmetrical axes, respectively, which are illustrated in Figs. 5 and 6 for the two mode-split geometries used. For either geometry, when a magnetic wall is applied, only the even mode or mode 1 is excited and the self-resonant frequency response is plotted using the dotted line, where the self-resonant frequency can be identified at a resonant peak. On the other hand, if an electric wall is applied, only the odd mode or mode 2 is excited and the simulated results are plotted using the broken line. Without applying any electric or magnetic wall, the simulation results show the split-mode frequencies, which are plotted using the full line. It is evident that the two split-mode frequencies for either geometrical perturbation are equal to the self-resonant frequencies, which confirms our above suggestion that there is no coupling between the two modes.

To this end, a circuit model for the two-pole dual-mode bandpass filters of Fig. 4 has been developed, which is shown in Fig. 7. There are four nodes, labeled with 0–3 in this circuit. Resonator 1 with a resonant frequency of $f_{01} = 1/2\pi\sqrt{L_1C_1}$ is used to represent mode 1 of a dual-mode triangular patch resonator; while resonator 2 represents mode 2 with a resonant frequency of $f_{02} = 1/2\pi\sqrt{L_2C_2}$. The two resonators are coupled, respectively, in parallel to the input and output (I/O) ports through the admittance inverters with characteristic admittances of $J_{0,1}, J_{1,3}, J_{0,2}$, and $J_{2,3}$. An extra inverter of $J_{0,3}$ is introduced to model the direct coupling between the I/O ports. A noticeable thing is that the circuit model does not have an inverter connected between nodes 1 and 2 so that there is no coupling between the two resonators. One can find that this circuit model is entirely different from that for the dual-mode square or circular patch resonator filters in which the main couplings are in a series structure.

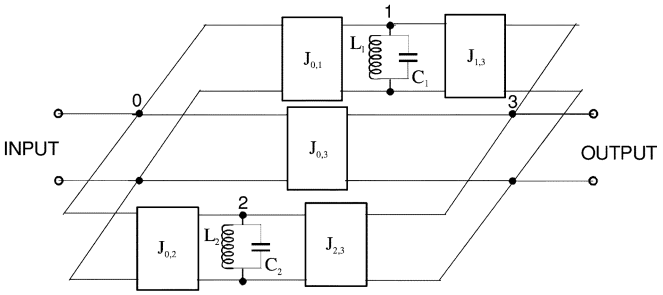

Fig. 7. Circuit model for two-pole dual-mode microstrip triangular patch resonator filters.

Two filters have been designed. The first filter (design 1) has a passband from 3995 to 4205 MHz, and is implemented with the structure of Fig. 4(a). With 50-Ω terminations, the circuit parameters are

$$f_{01} = 4320\,\text{MHz}$$
$$f_{02} = 4040\,\text{MHz}$$
$$J_{0,1} = 0.2355$$
$$J_{0,2} = 0.2500$$
$$J_{0,3} = 0.0125$$
$$J_{1,3} = J_{0,1}$$

and

$$J_{2,3} = -J_{0,2}.$$

where all the J values are normalized with the terminal admittance. The microstrip dual-mode triangular patch resonator has a size of $a = 15$ mm and $b = 11.25$ mm on a 1.27-mm-thick dielectric substrate with a relative dielectric constant of 10.8. The I/O coupling lines have a width of 1 mm and a gap of 0.25 mm to the patch resonator. Note that, in this design, mode 1 has a higher resonant frequency resulting from the small cut. $J_{1,3} = J_{0,1}$ and $J_{2,3} = -J_{0,2}$ are only feasible in this filter structure due to the symmetric field distribution of mode 1 and the antisymmetric field distribution of mode 2, respectively. Both theoretical analysis based of the circuit model of Fig. 7 and full-wave EM simulation using Sonnet ***em***[1] have been carried out. The results are plotted in Fig. 8(a), which not only demonstrate typical Chebyshev two-pole filter responses, but also show a good agreement between theory and EM simulation. This validates the proposed circuit model for this type of filter.

The second filter (design 2) is designed to have a passband from 3860 to 4020 MHz. The circuit parameters for this filter are give by

$$f_{01} = 3840\,\text{MHz}$$
$$f_{02} = 4040\,\text{MHz}$$
$$J_{0,1} = 0.20$$
$$J_{0,2} = 0.20$$
$$J_{0,3} = 0.02$$
$$J_{1,3} = J_{0,1}$$

and

$$J_{2,3} = -J_{0,2}.$$

[1]***em***, ver. 7.0, Sonnet Software Inc., Liverpool, NY, 2001.

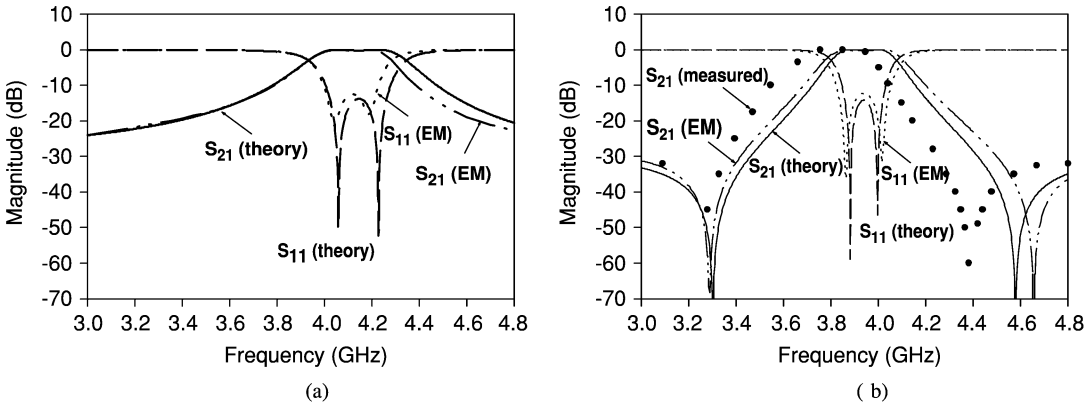

Fig. 8. Performance of two-pole dual-mode microstrip triangular patch resonator filters. (a) Design 1 based on the structure of Fig. 4(a). (b) Design 2 based on the structure of Fig. 4(b).

In this case, mode 1 has a lower resonant frequency and, hence, the filter structure of Fig. 4(b) should be used for the implementation. The resultant microstrip dual-mode triangular patch resonator has a size of $a = 15$ mm and $b = 14$ mm on a 1.27-mm-thick dielectric substrate with a relative dielectric constant of 10.8. Again, the I/O coupling lines have a width of 1 mm and a gap of 0.25 mm. Fig. 8(b) illustrates the frequency responses obtained by circuit modeling and EM simulation. It is interesting to note that this filter exhibits a quasi-elliptic function response with two transmission zeros at finite frequencies near the passband, resulting in a better selectivity as compared to the first filter design. The experiments were also carried out to confirm the dual-mode operation of this type of filter, and the measured results (S_{21} only for clarity) are also plotted as dotted points in Fig. 8(b).

Inspecting the two sets of design parameters for the two filters, the reason on the different frequency responses of Fig. 8 can be seen, which is mainly due to the different resonant frequencies of mode 1 in both filters. Also, the large difference in $J_{0,3}$ for the direct coupling between I/O will be accounted for. Since there is no coupling between the two modes, the mode frequencies can easily be controlled by the small perturbation to make the two modes split, while the I/O couplings are controlled by the coupled feed lines.

After the success in demonstrating the two-pole dual-mode microstrip triangular patch resonator filters, we have further developed multipole filters. Fig. 9 shows a photograph of a fabricated four-pole filter of this type on a RT/Duriod substrate with a relative constant of 10.8 and a thickness of 1.27 mm. The filter consists of two dual-mode microstrip triangular patch resonators in a very simple cascaded coupling structure. The filter was designed using the tool of full-wave EM simulation. The measured frequency responses of the filter are plotted in Fig. 10, which were obtained using an HP8720 network analyzer. The filter shows very good performance with a measured insertion loss of $\sim$2.3 dB at a midband frequency of 4.01 GHz. The selectivity on the low side of the passband would seem better than what is attainable for a direct-couple four-pole filter. This is due to an inherent (not designed) transmission zero on this side, which can clearly seen from the wide-band response of the filter. It is also interesting to see that the first spurious response occurs at approximately 6.45 GHz.

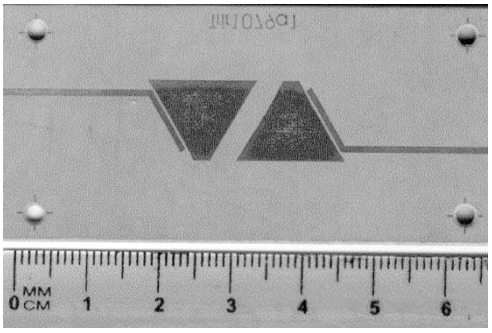

Fig. 9. Fabricated four-pole dual-mode microstrip triangular patch resonator filter.

Generally, for designing this type of filter with an order higher than two, the circuit mode of Fig. 7 can be extended to have a coupling scheme as shown in Fig. 11, where nodes 1–n represent n resonators and nodes 0 and $n + 1$ represent the I/O ports. Resonators 1 and 2 are realized with the dual modes in a dual-mode resonator, as are the other pairs of resonators. The couplings are represented by characteristic admittances $J_{i,k}$, as indicated. The synthesis of this type of filter can be done by optimization in *general* [20]. For demonstration, a four-pole filter of this type has been synthesized based on the coupling structure of Fig. 11 and the results for 50-Ω terminations are given as follows:

$$f_{01} = f_{03} = 4140 \text{ MHz}$$
$$f_{02} = f_{04} = 4002 \text{ MHz}$$
$$J_{0,1} = J_{3,5} = 0.24$$
$$J_{0,2} = J_{4,5} = 0.2$$
$$J_{1,3} = 0.075$$
$$J_{2,4} = -0.055.$$

The theoretical response of the synthesized filter, along with the simulated response of a practical filter similar to that of Fig. 9, is shown in Fig. 12, where a good agreement between the two can be observed. We also note that both theoretical and simulated responses show an inherent transmission zero on the low side of the passband for this filter, which has been confirmed experimentally in Fig. 10.

The unloaded Q of this type of resonator is expected to be similar to that of square patch dual-mode resonator. We have

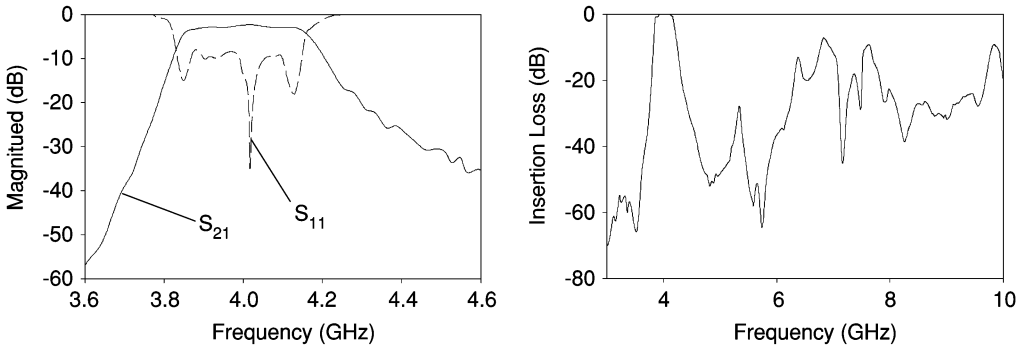

Fig. 10. Measured performance of the four-pole dual-mode microstrip triangular patch resonator filter of Fig. 9.

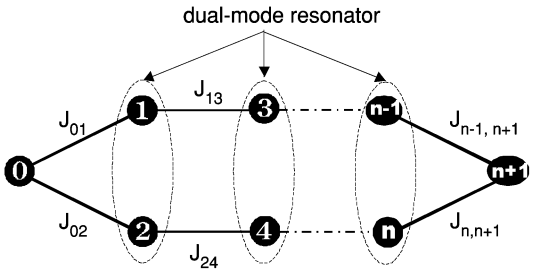

Fig. 11. Coupling configuration for multiorder dual-mode filters.

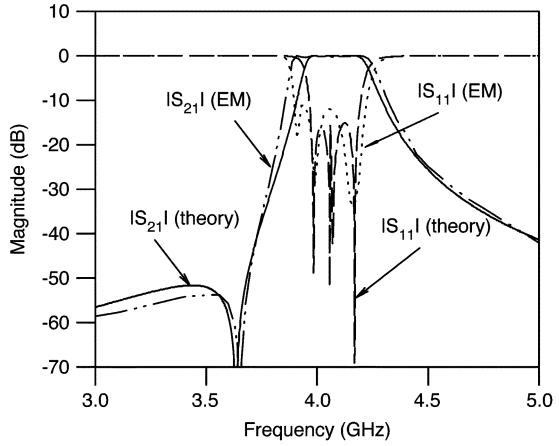

Fig. 12. Four-pole dual-mode filter response.

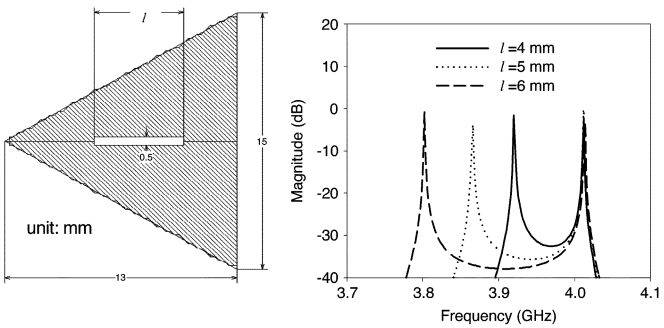

Fig. 13. Characteristics of mode splitting for a dual-mode triangular patch resonator perturbed with a narrow slit.

carried out full-wave simulations to extract the unloaded Q for the two modes of a triangular patch resonator having the dimensions given in Fig. 5. It turns out that the two modes also have a similar unloaded Q. Considering only the conductor loss by assuming a 10-μm-thick copper patch and a 10-μm-thick copper ground, we found that both modes have an unloaded Q of around 950. Further taking into account the dielectric loss by assuming a loss tangent of 0.002 for the dielectric substrate used, the simulated unloaded Q for both modes are approximately 320. For filter applications, the resonators should be assembled in a metal housing to eliminate the radiation loss.

It might be worth mentioning that there are methods for producing mode splitting other than those described above. For instance, Fig. 13 shows the simulated characteristics of mode splitting for a dual-mode triangular patch resonator perturbed using a narrow slit along its symmetric axis. For the simulations, the width of the slit was kept constant as 0.5 mm, while the length of the slit, i.e., l was changed from 4 to 6 mm. As can be seen from Fig. 13, the longer the slit, the larger the mode splitting. Again, it can be shown that the mode self-resonant frequencies coincide with the two split-mode frequencies. This indicates that the two split modes obtained in this way also do not couple each other. However, in this case, the simulations show that the self-resonant frequency of mode 1 is hardly changed against the variation of the slit length, implying the mode 1 is not perturbed. This can easily be explained in the light of the current distributions shown in Fig. 3, and the reason for this is that the slit is cut along the current flowing of mode 1 so it, in fact, does not perturb the field distribution of this even mode.

V. Conclusion

We have carried out an investigation into the dual-mode operation of microstrip triangular patch resonators and their applications in realizing dual-mode microwave planar filters. We have presented for the first time the theoretical solutions of a pair of fundamental degenerate modes of an equilateral patch resonator. It has been shown that the degenerate modes can result from the rotation and superposition of a fundamental mode. The characteristics of the dual modes and their mode splitting have been described. We have also demonstrated, for the first time, dual-mode microstrip triangular patch resonator filters. A circuit model has been also proposed for modeling this type of dual-mode filter. It has been shown that the triangular dual-mode patch resonator filter operates differently from the square or circular dual-mode patch resonator filter. It offers not only alternative designs, but also results in a compact size and simple coupling topology in a cascaded form. It is expected that

this type of filter will be very attractive for developing planar microwave filters with low loss and high power handling. It will also be promising for applications of high-temperature superconductor, RF microelectromechanical systems (MEMS), and low-temperature co-fired ceramic (LTCC) technologies.

REFERENCES

[1] J.-S. Hong and M. J. Lancaster, *Microstrip Filters for RF/Microwave Applications*. New York: Wiley, 2001.

[2] Y. Toutain, J.-P. Coupez, and C. Person, "Microstrip miniaturized loop-filters with high out-of-band rejection for future 3G mobile terminals," in *IEEE MTT-S Int. Microwave Symp. Dig.*, 2001, pp. 1589–1592.

[3] P. Blondy, A. R. Brown, D. Cros, and G. M. Rebeiz, "Low loss micromachined filters for millimeter-wave telecommunication systems," in *IEEE MTT-S Int. Microwave Symp. Dig.*, 1998, pp. 1181–1184.

[4] C. Y. Ng, M. Chongcheawchanman, M. S. Aftanasar, I. D. Robertson, and J. Minalgiene, "X-band microstrip bandpass filter using photoimageable thick-film materials," in *IEEE MTT-S Int. Microwave Symp. Dig.*, 2002, pp. 2209–2212.

[5] W. Hattori, T. Yoshitake, and K. Takahashi, "An HTS 21-pole microstrip filter for IMT-2000 base stations with steep attenuation," *IEEE Trans. Appl. Superconduct.*, pt. 2, vol. 11, pp. 4091–4094, Mar. 2001.

[6] G. L. Matthaei, "Narrow-band, band-pass filters with zig–zag, hairpin-comb resonators," in *IEEE MTT-S Int. Microwave Symp. Dig.*, 2002, pp. 1931–1934.

[7] K. F. Raihn and G. L. Hey-Shipton, "Folded dual-mode HTS microstrip band pass filter," in *IEEE MTT-S Int. Microwave Symp. Dig.*, 2002, pp. 1959–1962.

[8] I. Wolff, "Microstrip bandpass filter using degenerate modes of a microstrip ring resonator," *Electron. Lett.*, vol. 8, no. 12, pp. 302–303, June 1972.

[9] J.-S. Hong and M. J. Lancaster, "Microstrip bandpass filter using degenerate modes of a novel meander loop resonator," *IEEE Microwave Guided Wave Lett.*, vol. 5, pp. 371–372, Nov. 1995.

[10] J. A. Curitis and S. J. Fiedziuszko, "Miniature dual mode microstrip filters," in *IEEE MTT-S Int. Microwave Symp. Dig.*, 1991, pp. 443–446.

[11] R. R. Mansour, "Design of superconductive multiplexers using single-mode and dual-mode filters," *IEEE Trans. Microwave Theory Tech.*, vol. 42, pp. 1411–1418, July 1994.

[12] R. R. Mansour, B. Jolley, S. Ye, F. S. Thomson, and V. Dokas, "On the power handling capability of high temperature superconductive filters," *IEEE Trans. Microwave Theory Tech.*, vol. 44, pp. 1322–1338, July 1996.

[13] Z.-Y. Shen, C. Wilker, P. Pang, and C. Carter, "High-power HTS planar filters with novel back-side coupling," *IEEE Trans. Microwave Theory Tech.*, vol. 44, pp. 984–986, June 1996.

[14] M. A. Hein *et al.*, "High-power high-Q YB_aC_uO disk resonator filter," in *Proc. EUCAS Applied Superconductivity*, 1997, pp. 319–322.

[15] J.-S. Hong and M. J. Lancaster, "Microstrip triangular patch resonators filters," in *IEEE MTT-S Int. Microwave Symp. Dig.*, 2000, pp. 331–334.

[16] M. Cuhaci and D. S. James, "Radiation from triangular and circular resonators in microstrip," in *IEEE MTT-S Int. Microwave Symp. Dig.*, 1977, pp. 438–441.

[17] J. Helszajn and D. S. James, "Planar triangular resonators with magnetic walls," *IEEE Trans. Microwave Theory Tech.*, vol. MTT-26, pp. 95–100, Feb. 1978.

[18] J.-S. Hong and S. Li, "Dual-mode microstrip triangular patch resonators and filters," *IEEE MTT-S Int. Microwave Symp. Dig.*, pp. 1901–1904, 2003.

[19] J. Helszajn, *Microwave Planar Passive Circuits and Filters*. New York: Wiley, 1994.

[20] U. Rosenberg and S. Amari, "Novel coupling schemes for microwave resonator filters," *IEEE Trans. Microwave Theory Tech.*, vol. 50, pp. 2896–2902, Dec. 2002.

Jia-Sheng Hong (M'94) received the D.Phil. degree in engineering science from the University of Oxford, Oxford, U.K., in 1994. His doctoral dissertation concerned EM theory and applications.

In 1994, he joined the University of Birmingham, where he was involved with microwave applications of high-temperature superconductors, EM modeling, and circuit optimization. In 2001, he joined the Department of Electrical, Electronic and Computer Engineering, Heriot-Watt University, Edinburgh, U.K., as a faculty member leading a team for research into advanced RF/microwave device technologies. He has authored and coauthored over 80 journal and conference papers, and also *Microstrip Filters for RF/Microwave Applications* (New York: Wiley, 2001). His current interests involve RF/microwave devices, such as antennas and filters, for wireless communications and radar systems, as well as novel material and device technologies including RF MEMS and high-temperature superconducting devices.

Dr. Hong has served on the Editorial Board of the IEEE TRANSACTIONS ON MICROWAVE THEORY AND TECHNIQUES and on the IEEE Microwave Theory and Techniques Society (IEEE MTT-S) International Microwave Symposium (IMS) Technical Program Committee (TPC).

Shuzhou Li received the B.S. degree in physics from the Central South Institute of Mining and Metallurgy, Changsha, China, in 1982, and the M.S. degree in microelectronic devices and solid-state physics from Beijing Normal University, Beijing, China, in 1988.

In 1988, he joined the Peking University, Beijing, China, as a Research Engineer with the Institute of Microelectronics. Since 1990, he has been with the Institute of Acoustics, Chinese Academy of Sciences, Beijing, China, where he is currently a Senior Engineer. In 2002, he was on leave as a Visiting Scholar with the Heriot-Watt University, Edinburgh, U.K.